THz Time-Domain Spectroscopy on Ammonia

H. Harde and J. Zhao

Universität der Bundeswehr Hamburg, Holstenhofweg 85, 22043 Hamburg, Germany

M. Wolff, R. A. Cheville, and D. Grischkowsky[*]

School of Electrical and Computer Engineering and Center for Laser and Photonics Research, Oklahoma State University, Stillwater Oklahoma 74078, USA

Received: January 9, 2001; In Final Form: April 3, 2001

We use the technique of terahertz time-domain spectroscopy to experimentally and theoretically study the absorption and the dispersion of ammonia vapor. Our measurements show small deviations from the rotation-inversion spectrum which originate from transitions in the ν_2 hot band and from the $(NH_3)_2$ dimer. We investigate the molecular tunneling in ammonia and apply our new molecular response theory to analyze the inversion spectrum of this molecule. The theory includes the molecular response of polar molecules to an external electric field over the duration of a collision with the molecular response time as a control parameter, and it unifies the basic collision theories of Lorentz, van Vleck–Weisskopf, and Debye. The calculated absorption and dispersion based on this theory fits the measurements over the full spectral range of the THz spectrum and allows to determine a response time of the order of 100 fs.

I. Introduction

Ammonia was one of the pioneering species for the development of microwave spectroscopy and probably belongs to the group of the best known and most intensively investigated molecules in this spectral range.[1,2] Extensive studies were also performed in the frequency range above 3 THz (100 cm^{-1}) using Fourier transform techniques with classical far-infrared (FIR) light sources and bolometers as detectors. Only few measurements are known for the frequency range between which is of interest due to the observation of lines from the ν_2 hot band[3] and the troughs between rotational J-multiplets.[4] These spectra are of fundamental interest in astrophysics to study the composition and temperature of the atmosphere of planets like Jupiter or Saturn and to determine the ammonia concentrations in the interstellar space.

Although for high resolution investigations within narrow frequency intervals sub-mm wave oscillators, far-IR lasers and nonlinear mixing techniques can successfully be used to collect the relevant spectroscopic data, for broadband measurements over a wide frequency range in recent years only far-IR Fourier spectrometers with relatively low radiation power and low detection efficiency were available.

With the newly developed terahertz beam sources, producing subpicosecond pulses of THz radiation, a new and wide frequency range for time and frequency domain studies of materials and ranging experiments is available.[5–13] The pulses essentially consist of a single cycle over the pulse duration of typically 100–300 fs, and are characterized by a phase coherent, transform-limited white spectrum covering two decades of frequency from approximately 50 GHz up to more than 5 THz.[7] This frequency range, midway between the microwave and the infrared frequencies, is important owing both to the samples that can be investigated and to the unprecedented experimental conditions encountered with these THz pulses. We have used the powerful technique of THz time-domain spectroscopy[5–13] (THz-TDS) to investigate ammonia in a spectral range between 80 GHz and 2.5 THz with the objective to study the line-shape of inversion transitions.

Ammonia is distinguished by even (+) and odd (−) states, directly related to the symmetric and antisymmetric wave functions of a symmetric top. Given a wave function described by a superposition of the + and − states, the molecule can oscillate by tunneling of the nitrogen atom through the symmetry plane defined by the three hydrogen atoms.[1,2] The inversion corresponds to a transition between the + ↔ − states of the rotational levels, which are split into a doublet. Already at moderate pressures the line-width due to pressure broadening of such inversion lines is comparable to the center frequency at 23.8 GHz.

Standard collision theory predicts a line-shape for a pressure broadened line in this frequency range which is given by the van Vleck–Weisskopf theory[14] and is distinguished by a broad, constant absorption at the high-frequency side. However, such a constant absorption in the high-frequency wing is in disagreement with physical plausibility.

This discrepancy may be eliminated by applying our new molecular response theory,[12,13] which was developed for rotational transitions but also holds for the inversion lines. Compared to conventional collision theories,[14,15] it additionally includes the molecular response of polar molecules to an external electric field over the duration of a collision. In previous investigations of methyl halides,[12,13] the molecular response was observed as a deviation from classical line-shape theory[14,15] in the high frequency wing of the rotational absorption spectrum. For ammonia, these measurements directly relate to the inversion of molecules with the molecular response during a collision. Fitting the molecular response theory to our measurements allows determination of the molecular orientation time. With a response time of about 100 fs found from analysis of our measurements, and using this new line-shape, good agreement between experiment and calculation is obtained, although an

* To whom correspondence should be addressed. Phone: (405)-744-6622; FAX: (405)-744-9198; E-mail: grischd@ceat.okstate.edu.
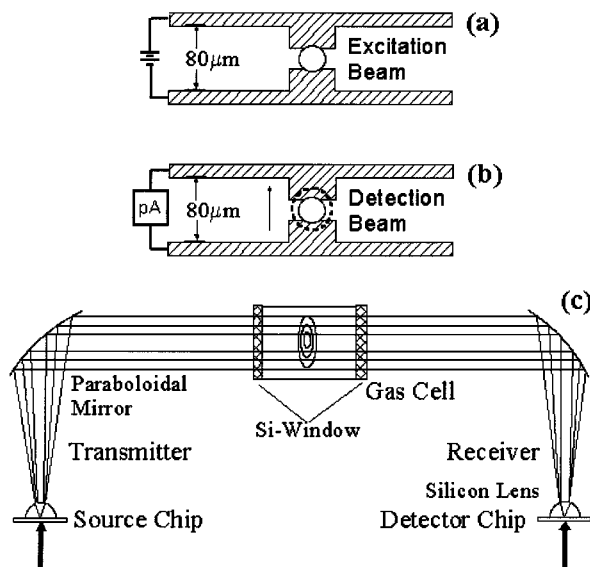
Figure 1. (a) Optoelectronic transmitting antenna used to generate pulses of THz radiation, (b) receiving antenna geometry, and (c) THz collimating and focusing optics together with a vapor cell.

accurate measurement of the inversion spectrum is complicated by the overlapping rotational band structure of the molecule which at its maximum is orders of magnitude larger.

With our THz technique the fact that a continuous band of frequencies can be monitored in a single measurement permits for the first time determination of the inversion line absorption over a frequency window which is only restricted and influenced by the overlapping rotational band structure. In addition, the wide bandwidth of THz-TDS allows us to distinguish almost 50 lines in the ν_2 hot band of ammonia at frequencies above 600 GHz superimposed on the rotation−inversion spectrum of the vibrational ground state. At 1.6 THz an additional broad absorption band is localized which we believe to originate from $(NH_3)_2$ dimers. To our knowledge, this is the first time that such a feature is observed at room temperature.

II. Experimental Setup

The optoelectronic THz system used for our experiments is shown in Figure 1. The key element for generating terahertz radiation is a photoconducting antenna chip or for some of the experiments a GaAs crystal plate with (110) orientation irradiated with 60−70 fs laser pulses coming at a rate of 100 MHz from a Ti:sapphire laser.

For measurements with increased sensitivity at lower frequencies, as this is of interest when studying the inversion lines, we used a dipole antenna fabricated on a GaAs wafer with a 5 μm gap and 80 μm length (Figure 1a). This antenna is DC biased at 5−10 V and generates pulses with a majority of the spectral energy density at frequencies between 200 GHz and 2 THz but still permits measurements to frequencies slightly below 80 GHz.

Alternatively to the dipole antenna, a 0.4 mm GaAs thick plate was used for generating the THz radiation by optical ractification.[16] With this transmitter THz pulses of similar quality and bandwith are obtained.

The emitted teraHz radiation is collimated by a silicon lens and paraboloidal mirror into a highly directional beam with a 25 mrad divergence. After a 50 cm propagation distance, this beam is focused by an identical combination of mirror and lens onto the receiving antenna (Figure 1b) which is fabricated on an ion-implanted silicon-on-sapphire wafer and consists of a coplanar transmission line structure with a 5 μm gap and 80

μm length. The electric field of the incoming terahertz pulses induces a voltage across the 5 μm wide antenna gap and is measured by photoconductively shorting the gap with laser pulses from a detection beam while monitoring the respective photocurrent in the antenna as a function of the time delay between the optical excitation and the probe pulses.

Three vapor cells, located as shown in Figure 1c, were used. Measurements optimizing sensitivity near the center of the rotational lines and avoiding spectrally dense samples were made in a short cell with a path length of 11 mm. For registration of the spectrum between the rotational lines, a medium sized cell of 172 mm length was applied, and to maximize sensitivity to the considerably weaker inversion absorption, a 380 mm path length cell was used. All cells were equipped with 10 mm thick high resistivity (10 $k\Omega$-cm) silicon windows. Silicon is an optimal window material, due to its almost complete transparency and lack of dispersion in the THz frequency range.[6] The entire THz system is located in an airtight enclosure to mitigate the effects of water vapor on the THz beams.[5]

The cells were filled with ammonia, and fitted with capacitance manometer gauges (MKS Baratron) to measure pressures in the range 0−3000 hPa (0−2300 Torr). The experimental cell was evacuated to < 0.1 Pa using a roughing pump between each series of measurements. Upon filling the cell, adsorption at the cell wall caused slight pressure drops over time. A metering valve was used to control cell pressures during data acquisition to ± 3.33 hPa (2.5 Torr). The gas was allowed time to come into thermal equilibrium with room temperature after each fill, and a thermocouple sensor accurate within 0.1 K monitored the cell temperature.

III. Measurements

We have used this optoelectronic THz system to perform time-domain spectroscopy of ammonia, a symmetric top molecule and an interesting candidate for studies of molecular collisions. THz-TDS requires two measurements of the pulse-shape, one without the vapor in the cell to determine the input pulse (reference pulse) and a second one with the vapor in the cell to register the interaction of the pulse with the sample.[6]

Figure 2 shows a measurement for 940 hPa of ammonia in the 11 mm long cell. Despite the short propagation length the input pulse (Figure 2a) is already slightly attenuated and reshaped at this pressure and changes to that represented in Figure 2b.

The spectrum (Fourier transform) of the input pulse which extends from low frequencies to about 2.5 THz is shown in Figure 2c as the upper curve (dotted line) in direct comparison with the spectrum of the pulse transmitted through the cell (solid line). The absorption and dispersion of the vapor is found from the ratio of these spectra or from fits of theoretical spectra to the measurements. Such calculated absorption for 940 hPa of ammonia and 11 mm cell length is represented in Figure 2d for the full rotation-inversion band structure together with the reference spectrum, indicating that only 4 lines ($J = 0-3$) fall into the spectral range of the antennas, whereas the strongest lines are far outside the covered THz spectrum. Nevertheless, these stronger lines still contribute to a broad background absorption in the measured range. Specifically at higher pressures this far-wing absorption can be comparable to the inversion absorption. Although in Figure 2d the first rotational line at 600 GHz still can be seen as a very small peak, the inversion lines are only visible on a magnified scale as represented by the inset showing the rotational line at the right and the 20× smaller broad inversion spectrum at the low-frequency side.
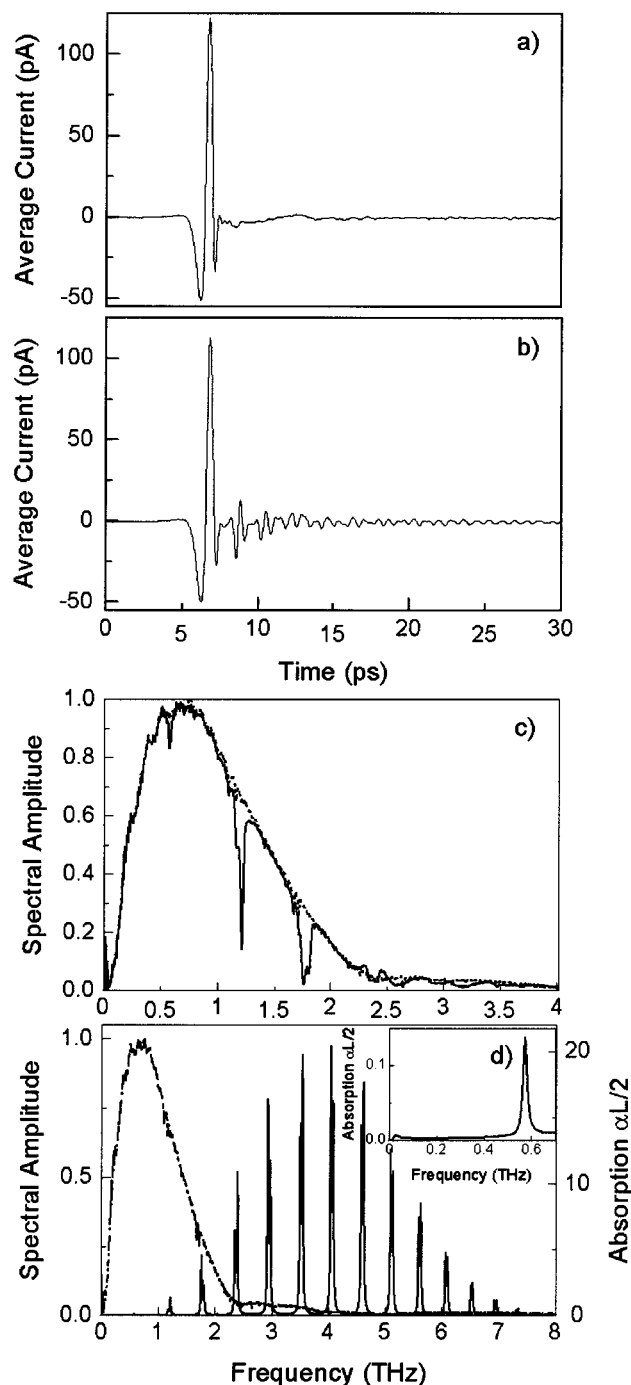
Figure 2. (a) Measured THz pulse without vapor in the cell (input pulse). (b) THz pulse after propagating through a 11 mm long gas cell filled with 940 hPa of ammonia vapor. (c) Fourier transform spectrum of the input pulse (upper curve, dotted line) and the transmitted pulse (solid line) of ammonia. (d) Rotation−inversion band structure of ammonia (solid curve) and reference spectrum (dash−dotted curve). The inset shows the low frequency wing of the absorption on an expanded scale. Note the small peak of the inversion lines at 0.024 THz with the absorption of approximately 0.01 and the first rotational transition at 0.58 THz ($J = 0$) with an absorption of 0.14.

At longer propagation lengths the vapor becomes opaque at the center of the stronger rotational lines but remains partially transparent in the troughs and at the low frequency wing of the rotation-inversion spectrum. Figure 3a shows a THz pulse which is strongly reshaped and attenuated after transmission through the 172 mm long vapor cell filled with 910 hPa of ammonia. Figure 3b represents the respective amplitude spectrum (solid line) together with the spectrum of the input pulse (dash−dotted
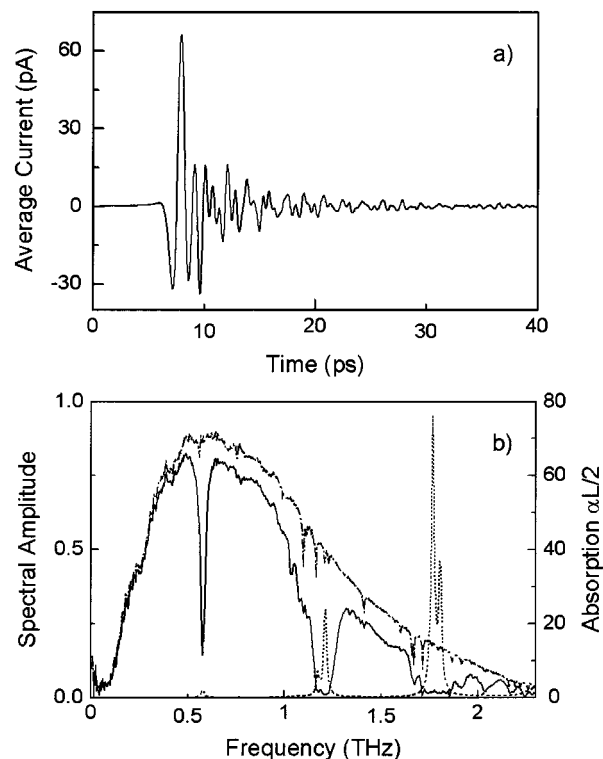

Figure 3. (a) Measured transmitted THz pulse through a 172 mm long gas cell filled with 910 hPa of ammonia vapor. (b) Fourier transform spectrum of the measured transmitted pulse (solid line), the reference spectrum (upper dash−dotted line) and calculated absorption (dotted line).

line), which shows some residual water vapor in the experimental enclosure (sharp dips), and the calculated absorption (dotted curve). The peak amplitude attenuation $e^{-\alpha L/2}$ (α − power absorption coefficient, L − absorption length) changes from e^{-2} for the first rotational line ($J = 0$) of the rotational manifold to e^{-76} for the third line ($J = 2$) and demonstrates the dramatic variation over this frequency range.

The spectral ranges with low absorption can be investigated most sensitively with the 380 mm long cell. This allows the observation of discrepancies between the pulse transmitted through the vapor and that calculated using published molecular constants. The spectrum of a measurement taken at a vapor pressure of 1000 hPa is shown in Figure 4a as the lower graph (solid line) together with the input spectrum (upper curve − dash−dotted line), which shows some residual water vapor lines. This figure also compares the calculated spectrum (dotted curve) of a pulse transmitted through the vapor and determined with the known molecular constants[17] of the rotation−inversion spectrum of the vibrational ground state.

Good agreement is obtained for frequencies less than 0.4 THz when considering the inversion and the wing absorption of the rotational lines. However, systematic deviations, measured as smaller transmissivity and, thus, higher absorption than those calculated, are found between the rotational transitions.

This discrepancy can be observed even more clearly at an increased pressure of 2000 hPa under otherwise same conditions. Figure 4b shows the respective Fourier transform spectrum of the measured pulse (solid line) together with the calculation (dashed curve). The additional absorption will be discussed in more detail in section V and can be explained to consist of individual weak lines classified as transitions in the ν_2 hot band, and a superimposed broad feature originating from the ammonia dimer.

THz Time-Domain Spectroscopy on Ammonia

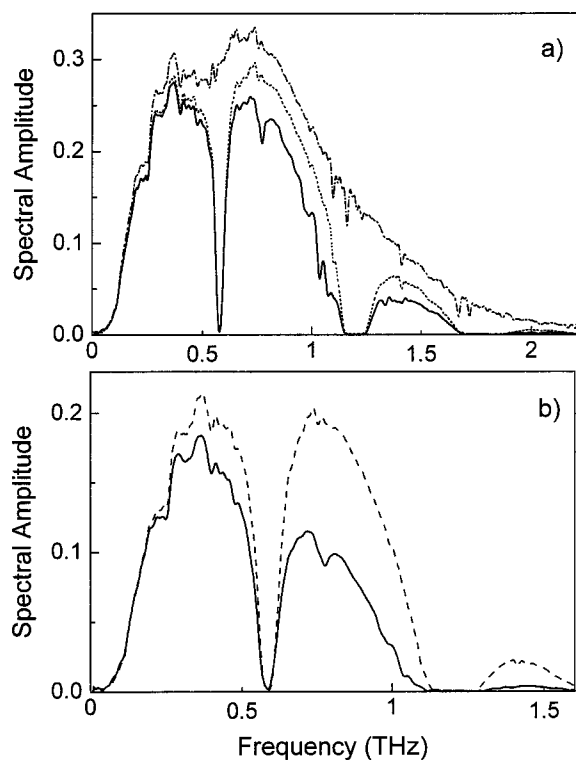*J. Phys. Chem. A, Vol. 105, No. 25, 2001* **6041**

Figure 4. (a) Fourier transform spectrum of the transmitted THz pulse through a 380 mm long gas cell filled with 1000 hPa of ammonia vapor (lower solid line), the respective simulation for a pulse neglecting the additional absorption (middle dotted curve) and reference spectrum (upper dash−dotted line). (b) Fourier transform spectrum of a pulse transmitted through 2000 hPa ammonia vapor (solid line) and respective calculation without additional absorption (dashed line).

While the line structure disappears at increased pressures due to pressure broadening of the lines, the overall additional absorption increases with pressure. At frequencies above 1.5 THz the vapor is completely opaque due to absorption from the rotational manifold.

An analysis of the measured data, particularly a quantitative interpretation of the inversion spectrum reflecting the molecular response requires precise modeling of the inversion-rotation band structure and also the additional absorption.

IV. Theory

In this section, we present the basic relations for calculating the inversion and rotation spectrum and review the molecular response line-shape theory[12,13] which applies for the rotational transitions as well as for the inversion lines. This theory includes the molecular response to an external electric field in the presence of molecular collisions. The new line-shape provides an improved fit to our measurements and avoids the nonphysical constant absorption in the high-frequency wing of a van Vleck− Weisskopf profile.

1. Rotation-Inversion Spectrum. Ammonia as a symmetric top molecule is of oblate form (pancake shape) with a moment of inertia along the principal axis smaller than that along the symmetry axis (z-axis) and therefore with a larger rotational constant B_V along the total angular momentum P than that along the z-axis with rotation constant A_V. Each rotational state with angular momentum P is characterized by the rotational quantum number J and consists of $2J + 1$ sublevels associated with the projection of the angular momentum P_z on the molecular symmetry axis and indicated by the projection quantum number K.
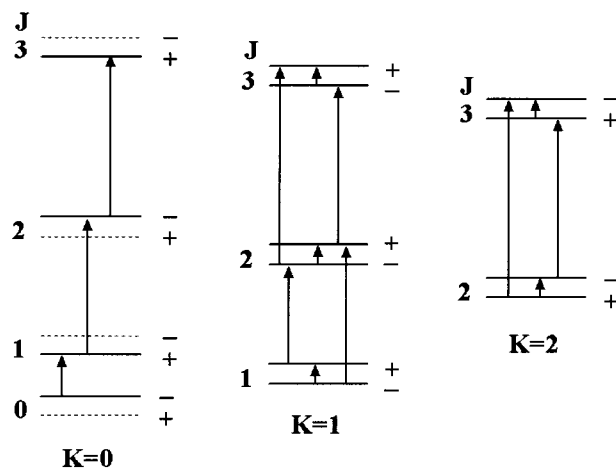

Figure 5. Level scheme of ammonia indicating the inversion and rotation transitions.

Additionally, for each J,K level with $K > 0$ two states of symmetry, $+$ and $−$ may be distinguished, directly related to the symmetry of the rotational wave functions. In a linear superposition of the $+$ and $−$ states the nitrogen atom can exist for some time on either side of the symmetry plane, which is defined by the three hydrogen atoms, before it switches to the inverse configuration, and the molecule is turned inside out.

Excitation of the molecules by the THz radiation induces transitions between pairs of J,K-levels of the lowest vibrational state, obeying the selection rules $+ \leftrightarrow −$, $\Delta J = 0, \pm 1$ and $\Delta K = 0$ as indicated in Figure 5 (see ref 1). For values of $K > 0$ the molecules can make electromagnetic transitions between the two states of symmetry, yielding the inversion spectrum with transitions $+ \leftrightarrow −$, $\Delta J = 0$, $\Delta K = 0$. They can also undergo transitions with $+ \leftrightarrow −$, $\Delta J = \pm 1$ and $\Delta K = 0$ which determine the rotational spectrum.

For $K > 0$ each rotational J,K level is split by the inversion frequency which for ammonia is $\omega_{0i}/2\pi = 23.8$ GHz.[1,2] Therefore, the rotational lines except those with $J = 0$ are split by twice this frequency. Because of centrifugal stretching of the molecule with increasing rotation frequency the rotational states are shifted, which is observed as a slight anharmonicity in the line spacing of the rotational lines and the removal of the K-degeneracy as well as a variation of the splitting between adjacent inversion states. Therefore, the inversion lines are no longer degenerate, but spread over a spectral interval of about 10 GHz.

At pressures above 100 hPa, however, due to pressure broadening the individual lines are no longer distinguishable and the inversion spectrum appears as a single broad line with a center inversion frequency ω_i. Also, all K-transitions ($K = 0 − J$) of a rotational line with the same rotational quantum number J can be considered as a single component represented by an average $\bar{K}$. For $J > 0$ then two components of a rotational line with frequencies

$$\frac{\omega_r^{\pm}(J)}{2\pi} = 2(J + 1)(B_V - D_{JK}\bar{K}^2) - 4D_J(J + 1)^3 \pm \frac{\omega_i}{2\pi} \quad (1)$$

can be distinguished. B_V is the rotational constant of the vibrational ground state about the total angular momentum and D_J and D_{JK} are the respective centrifugal stretching constants.[17]

The absorption coefficient for an individual inversion-rotation transition can be calculated as (for details see refs 1 and 13)

$$\alpha_{JK}(\omega) = \frac{\pi}{6nc\epsilon_0 h}|\mu_{JK}|^2 N_{JK}[1 - e^{-h\omega_L/2\pi kT}]\omega g_\alpha(\omega,\omega_L) \quad (2)$$

with $\omega_L = \omega_i$ for an inversion transition and $\omega_L = \omega_r^\pm(J)$ for a rotation transition. The term in brackets stands for the difference in the population between the lower and upper states. μ_{JK} is the average dipole matrix element for unpolarized radiation and/or unoriented molecules (including the transitions from the $2J + 1$ magnetic sublevels). N_{JK} represents the population per unit volume of the lower rotational state, n is the nonresonant refractive index, c is the speed of light, ϵ_0 is the vacuum permittivity, h is Planck's constant, and kT is the thermal energy.

The results of molecular response theory are summarized in $g_\alpha(\omega,\omega_L)$, which is a general absorption line-shape function of the form[12]

$$g_\alpha(\omega,\omega_L) = \frac{\Delta\omega_L}{(\omega - \omega_L)^2 + (\Delta\omega_L/2)^2}f_\alpha^+ -$$
$$\frac{\Delta\omega_L}{(\omega + \omega_L)^2 + (\Delta\omega_L/2)^2}f_\alpha^- \quad (3)$$

It differs from the standard Lorentzian[15] form by being multiplied by an additional shape factor, the switching function f_α^+ for the positive resonance term and a similar factor f_α^- for the "negative" frequency resonance term. For $f_\alpha^\pm = 1$, eq 3 is a pure Lorentzian, whereas for $f_\alpha^\pm = \pm\omega/\omega_L$ it assumes the van Vleck−Weisskopf shape. These switching functions come from the new molecular response theory and will be discussed in more detail in section IV.2. The width of a line is determined by the collisional dephasing time T_2 equal to the meantime between collisions, which for further distinction between inversion and rotation transitions is replaced by $\tau_L = 2/\Delta\omega_L$ $(L = i,r)$ with the angular frequency line-width $\Delta\omega_L$ of an inversion or rotation transition.

The change of the wave vector is given by[13]

$$\Delta k_{JK}(\omega) =$$
$$\frac{\pi}{3nc\epsilon_0 h}|\mu_{JK}|^2 N_{JK}(1 - e^{-h\omega_L/2\pi kT})\frac{\omega\omega_L}{\omega_L^2 - \omega^2}\cdot g_k(\omega,\omega_L) \quad (4)$$

where $g_k(\omega, \omega_L)$ is a general dispersion line-shape function of the form

$$g_k(\omega,\omega_L) = 1 - \frac{\Delta\omega_L^2}{8\omega_L}\left\{\frac{(\omega_L + \omega)}{(\omega_L - \omega)^2 + (\Delta\omega_L/2)^2}f_k^+ + \frac{(\omega_L - \omega)}{(\omega_L + \omega)^2 + (\Delta\omega_L/2)^2}f_k^-\right\} \quad (5)$$

and $f_k^\pm$ are the respective switching functions (presented in section IV.2) of the dispersion.

The power absorption coefficient $\alpha(\omega)$ and change of the wave vector $\Delta k(\omega)$ over the spectral range of the THz pulse are found by summing over all the inversion and rotation transitions.

2. Line-Shape Considerations and Molecular Response Theory. The overall absorption and dispersion are determined by the line-width and shape of the transitions, which contain information on the collision behavior as well as on the intermolecular forces. For optical and infrared transitions, it is well-known that the simple Lorentzian line-shape provides excellent agreement with experiment, particularly for the central region of the line. As the frequencies are reduced to those of the microwave or far-infrared region, and under conditions when a line-width becomes comparable with the transition frequency, the absorption profile of a collision broadened line is better represented by a van Vleck−Weisskopf line-shape. Also for the limiting case of zero transition frequency, the absorption and dispersion is described by the van Vleck−Weisskopf theory, which then converges to the Debye theory.[18]

The difference between the Lorentz and the van Vleck− Weisskopf theory is that the response of a molecule to an external field is only considered in its two limiting cases. While Lorentz assumed that directly after a collision molecules are oriented randomly with respect to the driving field and therefore no macroscopic polarization in the sample will be found, van Vleck and Weisskopf applied Boltzmann's statistics, assuming instantaneous realignment during a collision such that the molecules are oriented as to have a low energy in the field. A distribution in accordance with the Boltzmann law can be expected when the collision duration is short compared to the period of oscillation of the field. However, when the variations of the field become faster than the collision duration time or faster than any time response of molecules to the impressed field, thermalization cannot be established over the collision, and the original approximation of Lorentz becomes more realistic.

The frequency range where the transition between the two theories occurs indicates the duration of the collision or the molecular response time τ_C. This frequency range is completely covered by the spectrum of the THz pulses and therefore can be investigated by THz-TDS.

It is obvious that a more inclusive line-shape theory, which is applicable over the full spectral range, needs to include the temporal response of molecules to the field. We have derived such a molecular response theory.[12,13] Inclusion of the molecular response results in a time dependent and therefore also frequency dependent extra polarization of the vapor which may be formed over the collision duration time. This extra polarization results from the tendency of molecules to orient their dipole moment parallel to the field, as was considered in the van Vleck− Weisskopf case, but in the molecular response theory, the orientation is not assumed to be instantaneous. In the frequency domain, the magnitude of this extra polarization is determined by the frequency detuning of the field from the transition frequency compared to the reciprocal of the molecular response time τ_C. The polarization can vary from zero when frequency detuning is large compared to the inverse response time (Lorentz case) to a maximum polarization representing thermal equilibrium when the frequency detuning is small compared to the inverse response time (van Vleck−Weisskopf case).

This extra polarization modifies the absorption and dispersion of the vapor giving rise to small corrections in the wing of a spectral line. The faster the response of molecules, the more these contributions are shifted to the far wing of a line up to the limit of instantaneous response which is the van Vleck− Weisskopf case. From molecular response theory, we find a generalized line-shape of the type given by eq 3 for the absorption and by eq 5 for the dispersion. The switching function for absorption assumes the form

$$f_\alpha^\pm(\omega,\omega_L) = 1 - \frac{\omega_L \mp \omega}{\omega_L} \times \frac{1 + \Delta\omega_L\tau_C/2}{1 + (\omega_L \mp \omega)^2\tau_C^2} \quad (6)$$

whereas that for the dispersion is given by

THz Time-Domain Spectroscopy on Ammonia

J. Phys. Chem. A, Vol. 105, No. 25, 2001 **6043**

$$f_k^{\pm}(\omega,\omega_L) = 1 - \frac{\omega_L \mp \omega}{\omega_L} \times \frac{1 - 2(\omega_L \mp \omega)^2 \tau_C / \Delta\omega_L}{1 + (\omega_L \mp \omega)^2 \tau_C^2} \quad (7)$$

where τ_C is the molecular response time. These functions control the transition between the two basic line-shapes and describe the admixture of a van Vleck–Weisskopf profile to a Lorentzian as a function of the frequency detuning from resonance. An inspection of the switching functions shows that in the limit $(\omega_L \mp \omega)^2 \tau_C^2 \gg 1$, $f_a^{\pm} \to 1$, and the generalized line-shape function becomes the well-known Lorentzian for absorption, whereas $f_k^{\pm} \to 1 + (\omega_L \mp \omega)\tau/\omega_L\tau_C$. Conversely, when $(\omega_L \mp \omega)^2 \tau_C^2 \ll 1$, $f_{k,a}^{\pm} \to \pm \omega/\omega_L$ and the van Vleck–Weisskopf line-shape is obtained.

As a concluding remark, it is to be noted that molecular response theory would be especially applicable to recent far-infrared measurements in the troughs between the J rotational lines of ammonia and mixtures of ammonia and hydrogen.[4] Here, the fact that for molecular response theory the line-shape smoothly varies from van Vleck–Weisskopf to mixtures of van Vleck–Weisskopf and Lorentzian and then to Lorentzian as the frequency is increased for the increasing J rotational lines could help to resolve the discrepancies between the measured absorptions and calculations based on Lorentzian and Rosenkrantz line-shapes. This is especially true for trough absorptions with frequencies below 120 cm^{-1}. For frequencies above 120 cm^{-1}, the observed trough absorptions become less than Lorentzian and in better agreement with Ben-Reuven and Rosenkrantz theory.[4]

V. Discussion of Results

An analysis of the measurements presented in section III was performed by Fourier transforming the measured pulse structures into the frequency domain and comparing them with theoretical spectra. Additionally, the analysis can be done in the time domain by simulating the pulse structures and comparing them directly with the measurements. This time-domain calculation checks the self-consistency of the theory in that a strong comparison with the calculated indices of refraction are performed by the comparison of calculated pulses with the measurements. In both cases, first the absorption and dispersion of the vapor have to be calculated with the known molecular constants using the theoretical framework presented in the previous section. Multiplication of these spectra with the Fourier transform of the input pulse gives the transmitted amplitude absorption and dispersion spectrum behind the vapor. The inverse numerical Fourier transform of the calculated absorption and dispersion spectra yield the predicted output pulses transmitted through the vapor.

To successfully fit our experimental results, we must address all aspects of the theory reviewed in section IV and identify the additional absorption observed as deviation from the rotation–inversion spectrum. First, the pressure broadened line widths of the rotational transitions have to be determined as one of the significant parameters for modeling the rotational absorption band and their influence on the low-frequency wing of the spectrum. The second step is to explain and to classify the additional absorption in the central part of the spectrum because an exact modeling of this absorption is the prerequisite for a further quantitative analysis of the measurements. The final analysis is focused on molecular tunneling to obtain the line-shape of the inversion lines and to derive from this contribution the molecular response or orientation time τ_C.

1. Rotational Line-Width. At low pressures up to several 10 hPa, individual K-transitions belonging to the same lower
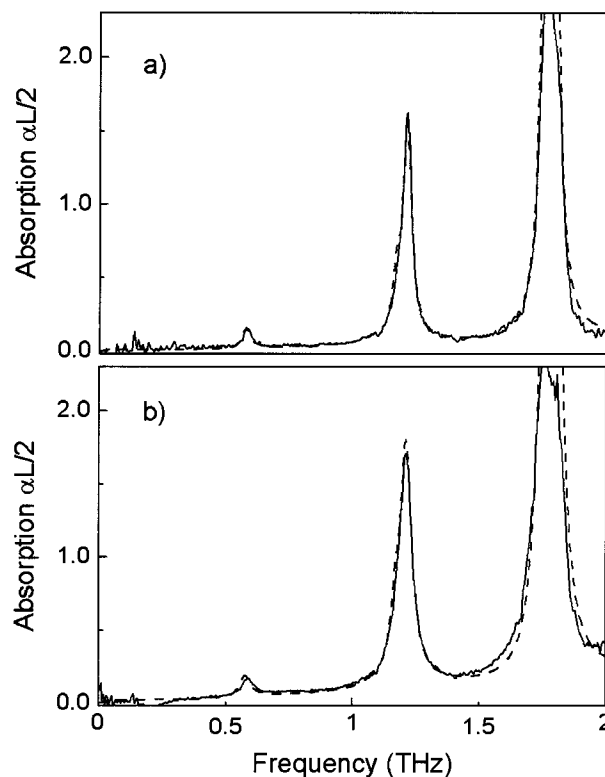

Figure 6. (a) Measured (solid line) and calculated absorption (dashed line) for 2000 hPa and (b) for 2950 hPa of ammonia at a cell length of 11 mm.

state rotational quantum number $J > 0$ may still be distinguished. Then the line-width of the J,K rotational lines is well represented by an empirical formula of Brown and Peterson[19] showing a relatively strong dependence of the width with the quantum numbers. At pressures of 1000 hPa or more, the range which is of interest for our investigations, an average over all K-transitions forming a rotational line is observed.

The line broadening is determined by a measurement of the type shown in Figure 2 using a short cell length which permits observation of the shape of the lower rotational lines without saturation as long as the gas is not completely opaque at the center frequencies of these lines. However, not only the lines falling into the covered spectral range of the THz pulses (see Figure 2), but also the higher lying transitions determine the measured absorption because the overlap of the wings of these strong lines cause an additional contribution in the observed spectral range. The size of this far wing absorption which sensitively depends on the line-width of the transitions, can be of comparable order as the inversion lines in this region. Therefore, it is important to monitor the line-width and any variations with J and to extrapolate to the strong lines ($J = 3-10$) which cannot directly be detected.

For an analysis of such measurement, the experimental absorption is directly compared with the theoretical amplitude absorption $\alpha(\omega)L/2$, obtained using the method outlined in section IV-1. Figure 6a shows the measured absorption (solid line) together with that calculated (dashed curve) for 2000 hPa of ammonia at a cell length $L = 11$ mm, and Figure 6b represents the respective spectra for 2950 hPa. It is to be noted that the peak absorption strength does not increase with pressure, but that the effect of the increasing pressure is to broaden the lines.

Because our experiments were performed at pressures where all K-transitions with the same rotational quantum number J
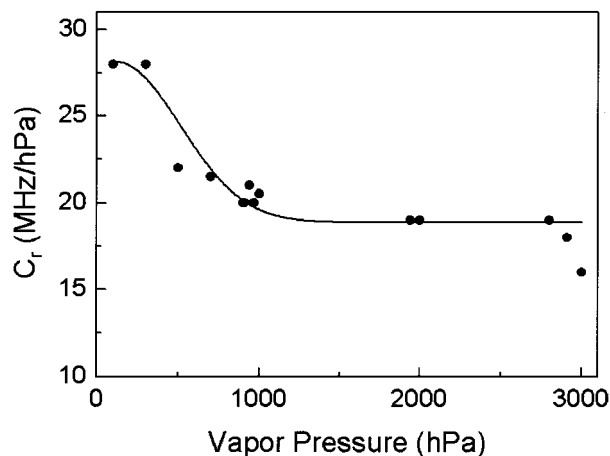
Figure 7. Pressure broadening coefficient C_r of the ammonia rotational lines at room temperature as a function of the vapor pressure.

TABLE 1: Calculated Averaged Collision Broadening Parameters for the Rotational Lines with Quantum Numbers $J = 0-10$ after Refs 19 and 20

J	$C_r(J)$ (MHz/hPa)	J	$C_r(J)$ (MHz/hPa)
0	21.7	6	27.8
1	20.1	7	25.5
2	30.2	8	23.7
3	27.8	9	22.5
4	29.0	10	22.5
5	27.2		

and symmetry merge into a single line, weighted averaged line widths $\Delta\bar{\omega}_L(J)$ were used in the calculation of absorption $\alpha(\omega)$ and change in the wave vector $\Delta k(\omega)$. These weighted averages were taken as follows[2]

$$\Delta\bar{\omega}_L(J) = \frac{\sum \Delta\omega_L(J,K)I_{J,K}}{\sum I_{J,K}} \qquad (8)$$

where $I_{J,K}$ is the intensity of line J,K and $\Delta\omega_L(J,K)$ is the corresponding line-width. The averaged line widths were obtained from the following literature values of the low-pressure full-width at half-maximum (fwhm) line widths as follows. For the inversion lines, Bleaney and Loubser[2] give an averaged pressure broadening parameter (fwhm collisional line-width per pressure p) $C_i = \Delta\bar{\omega}_i/2\pi p = 1.24$ cm^{-1}/atm = 36.7 MHz/hPa. For the $J = 0$ rotational line, Belov et al.[20] give a fwhm broadening parameter $C_r(J = 0) = \Delta\bar{\omega}_r(0)/2\pi p = 28.8$ MHz/ Torr = 21.7 MHz/hPa, and for the $J = 1-10$ rotational lines the weighted averages for the fwhm collision broadening were evaluated using the numerical data obtained from previous measurements[19] and given in Table 3 of ref 19. The results together with the parameter for $J = 0$ are listed in Table 1.

As long as the vapor pressure is less than 300 hPa, measurements and calculations agree well within the covered frequency range using the weighted average values for the collision broadening. At higher pressures, however, the broadening parameters are changing with pressure, as illustrated in Figure 7. Although the dots represent averaged values derived from fits to two or three individual measurements at a specific pressure, the solid line is a nonlinear fit to the data points of Figure 7. Because of the increasing opacity of the vapor with increasing frequency and due to the limited frequency resolution only the line widths of the first three rotational lines can be deduced from our data. For these lines, no different widths can be distinguished, and therefore a J-independent broadening coefficient C_r is introduced, as shown in Figure 7. This variation
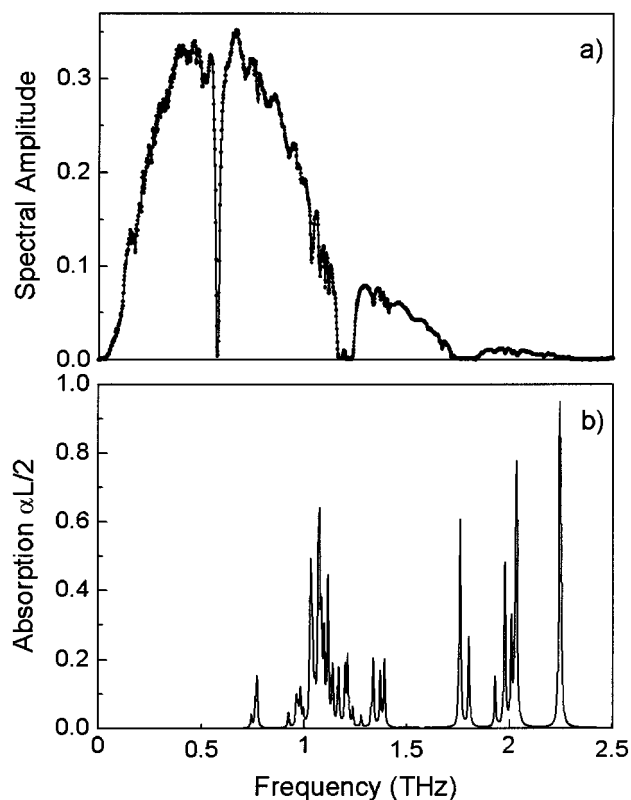

Figure 8. (a) Fourier transform of the measured transmitted pulse (dots) through 300 hPa of ammonia vapor at a cell length of 380 mm and calculation (solid curve) including the hot band line spectrum. (b) Calculated absorption of the hot ν_2 rotational band.

of C_r with pressure is due to simultaneous collisions with more than one collision partner.[2,21]

2. Additional Absorption. The 11 mm cell is too short to allow observation of the small inversion line absorption from which we expect information on the line-shape and the response of molecules. Such a contribution can be measured when using the longer vapor cells because the absorption $\alpha(\omega)L/2$ increases linearly, and the transmitted signal through the vapor decreases exponentially with increasing cell length. However, as already observed in Figure 4, with higher sensitivity not only the inversion in the low-frequency wing but also an additional weak absorption in the troughs between the rotational lines is monitored which cannot be explained by the rotation-inversion spectrum of section IV.

The deviations from theory show up as additional individual lines mainly in the spectral range between 0.7 and 1.5 THz, and as a continuous broad absorption band centered around 1.6 THz.

The additional lines are best observed when performing a measurement at reduced vapor pressure and using the 380 mm cell. Figure 8a shows the respective transmission spectrum of an input pulse propagated through 300 hPa of ammonia vapor at a temperature of 294 K (dots). All the observed lines appearing as small dips besides the rotational and water lines can be identified as transitions in the ν_2 vibrational state with an energy of 932.4 cm^{-1} above the molecular ground state (for these hot band transitions, see e.g., HITRAN Data Base[22]). At this temperature, 1% of the molecules are found in this excited state. Figure 8a also compares the experiment with a calculation (solid line), which was performed with the additional line spectrum represented in Figure 8b. For this calculation, 48 hot band transitions were considered within the frequency range from 0.7 to 2.3 THz assuming a pressure broadened line-width
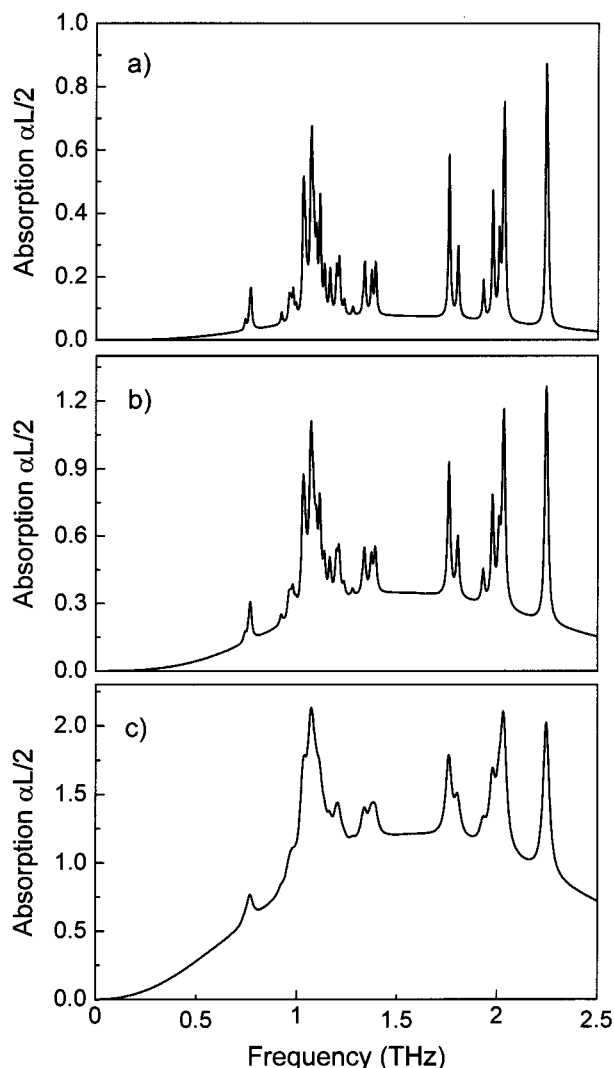
THz Time-Domain Spectroscopy on Ammonia

J. Phys. Chem. A, Vol. 105, No. 25, 2001 **6045**

Figure 9. Calculated hot ν_2 band and dimer absorption of ammonia vapor at (a) 500 hPa, (b) at 1000 hPa, and (c) at 2000 hPa for a 380 mm long gas cell.

$0.85\times$ that of the ground-state rotational transitions. Although the strongest lines are about 1 order of magnitude smaller than the weakest ground state rotation line ($J = 0$), the excellent agreement between measured and calculated spectra in Figure 8a can only be obtained with this correction.

With increasing temperature also the strength of the hot band transitions is expected to increase. This was checked by heating the vapor cell to 98 °C (371,2 K) and measuring the vapor absorption. Although at the higher temperature the population difference between the lower and higher states of these transitions is decreasing by about 20%, the absolute population is raised from 1% up to 2.7%. Therefore, the absorption depth of the hot band transitions is increasing about two times in good agreement with the observations.

At a vapor pressure of 300 hPa or less, the additional broad absorption structure is not observable; at higher pressures, however, this contribution is rapidly increasing. Figure 9 shows this continuous broad shoulder together with the line structure as derived from fits to the measurements at (a) 500, (b) 1000, and (c) 2000 hPa.

Because of the high purity of the ammonia vapor used in our experiments, a foreign species causing this additional broad absorption can be excluded. On the contrary, it is obvious that within some limits this contribution increases more rapidly than

other features of the spectrum. This suggests a pressure induced absorption process which is only observed under strong perturbations due to collisions, or the formation of a species which may exist at higher pressures and contributes to this absorption. Because no ammonia transitions and also no forbidden transitions in this spectral range are known, we believe that this continuous absorption originates from ammonia dimers $(NH_3)_2$ which are formed during a collision of two ammonia molecules and only may exist a few ps. As a confirmation of this hypotheses, we see that the background absorption is reduced by about 40% when increasing the vapor temperature from room temperature to 90 °C. The higher temperature impedes the formation of dimers because the thermal energy of the ammonia molecules acts against any attractive forces.

The number of transient dimers is expected to increase with the number of collisions and therefore with the pressure, and the relative number is expected to be of the order of the ratio of the collision time τ to the time Δt between collisions. For molecules at thermal velocities (660 m/s) and collision parameters of the order of a few Å, typically collision times of about 1 ps are estimated. The average time between collisions is determined by the reciprocal of the pressure broadened linewidth which at 1 atm is about 20 GHz and thus $\Delta t \approx 50$ ps. Therefore, the concentration of dimers should be of the order of a few %. On the basis of this simple picture, the relative percent of dimers with respect to the monomer concentration is expected to increase linearly with pressure, as long as multiple collisions can be neglected and the line-width is increasing linearly with pressure. Consequently, the absolute number is then growing quadratically with pressure, and the same applies to the dimer absorption, as observed in Figure 9.

Dimers are distinguished by additional degrees of freedom like the rotation or vibration of the two ammonia molecules against each other or a rotation of the dimers along their principal axes.[23,24] All these degrees of freedom can contribute to additional transitions and the interaction with electromagnetic radiation. Particularly, an excitation of the rotational mode is of further interest. From a simple picture we expect that a dimer has a moment of inertia which is about $6\times$ larger than that of an ammonia molecule and accordingly its rotational constant is this factor of 6 smaller than the rotation constant of NH_3 with $B_V = 298$ GHz. Because any rotation will not last much longer than the 1 ps collision time τ approximately equal to the lifetime of the dimers, the line-width of any transition cannot be defined sharper than $\Delta \nu \approx 1/\pi\tau$. Therefore, a continuous broad feature smearing out over approximately 1 THz can be expected.

The continuous absorption shown in Figure 9 with a width of about 1.7 THz and the maximum at 1.6 THz was simulated assuming a rotational band structure with a rotation constant $B_V = 50$ GHz and a line-width of several hundred GHz. Using a dipole moment of 0.75 D as this is known for the ammonia dimer,[23] a fit to the measurement gives excellent agreement when for the 500 hPa measurement the dimer concentration is assumed to be 2.1% and for the 1000 hPa measurement 5%. At pressures of 2 atm (2026 hPa) or more, an extending contribution at the low-frequency side of the continuous absorption is observed causing a further broadening of the absorption and a slight overall shift to lower frequencies. Including this additional contribution as this was done for the simulation shown in Figure 9c, the dimer concentration at 2000 hPa is 13% in acceptable agreement with our expectations.

At higher pressures, a dimer absorption also might be expected in methyl halides which have similar or even larger dipole moments. However, such contribution is expected to
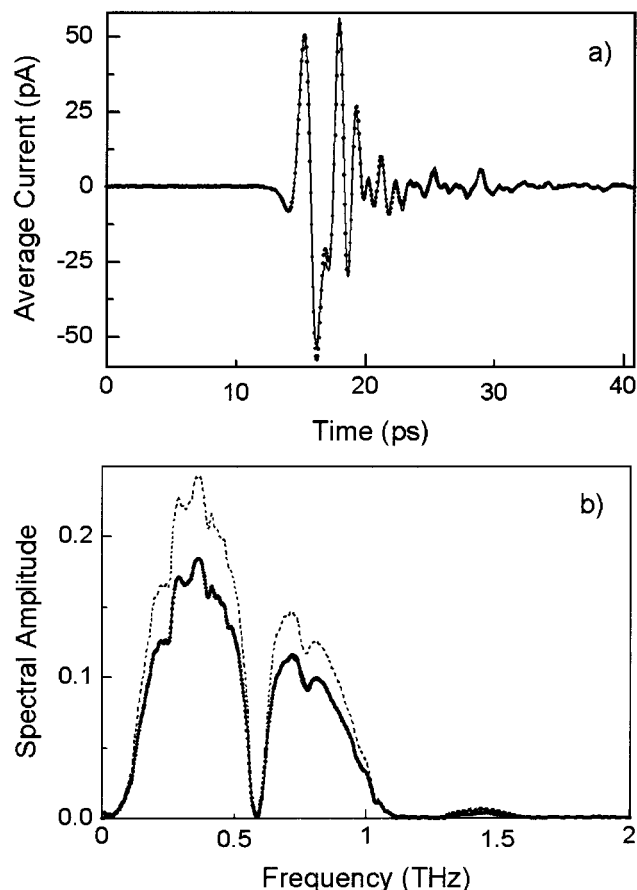
Figure 10. (a) Measured pulse (dots) transmitted through 2000 hPa of ammonia vapor at a cell length of 380 mm and calculated pulse (solid line) including the inversion. (b) Fourier transform of the measured pulse (dots) (see also Figure 4b), calculated spectrum including the hot band and the dimer absorption, but neglecting the inversion (upper dashed curve), and calculation including the inversion spectrum (solid graph).

overlap with the monomer spectrum, which is much more closely spaced and without any troughs left at the higher pressures. Therefore, under such conditions it is almost impossible to identify any dimer contribution.

3. **Molecular Tunneling.** The THz beam system, which at the low frequency side of the spectrum can be applied down to frequencies of approximately 60 GHz, does not allow the observation of the inversion line structure directly at its transition frequency of 23.8 GHz, which with increasing pressure even shifts to smaller frequencies. At the higher pressures, however, these transitions are strongly broadened extending up to frequencies which are covered by our THz system and thus permit measuring the high-frequency wing of the inversion spectrum as a broader background absorption and dispersion. This contribution can be identified when comparing a measurement with a calculation performed with and without the inversion lines.

For 2000 hPa ammonia vapor the transmitted pulse through the 380 mm cell is shown in Figure 10a as the measured dots in direct comparison with the calculated pulse (solid curve) which with the inversion included almost completely overlaps the measurement and demonstrates the excellent agreement between theory and experiment as well as the feasibility to directly analyze the data in the time domain. The respective transmission spectrum of the measurement already shown in Figure 4b is again represented in Figure 10b by the dots together with a simulation calculated without the inversion (upper curve

− dotted line) and including the inversion spectrum (solid line). This figure demonstrates the influence of the inversion over the full observed spectrum. From the fit to measurements,, we obtain a broadening parameter C_i consistent with the collision line-width given by Figure 7.

Such fit also shows a well observable shift of the inversion frequency ν_i to smaller frequencies with increasing pressure. Although the inversion transition cannot be monitored directly, the splitting of the rotational lines with $2\nu_i$ or the shift of the first rotational line ($J = 0$) can sensitively be measured. The first rotational line is shifted by ν_i to lower frequencies from the position calculated from the rotational constants. However, in contrast to ref 2 the shifted frequency is still far away from zero at 2 atm. From our measurements, we find an inversion frequency $\nu_i \approx 13(2)$ GHz at 2 atm and 8(3) GHz at 3 atm assuming the literature values[17] for the rotational constants ($B_V = 298.1$ GHz, $D_J = 25.2$ MHz, and $D_{J\,K} = -46.9$ MHz). Even 6 GHz larger values at these pressures are obtained, when the rotational constants B_V and D_J are also fitted with $B_V = 302$ GHz and $D_J = 350$ MHz. A further increase of ν_i by about 2 GHz is observed when increasing the temperature of the vapor by 70 K. It is to be noted that the frequency shift of the $J = 0$ line at low pressures has been measured to be 6.1 MHz/Torr[20] which corresponds to a shift of 9.27 GHz at two atm in reasonable agreement with our observations.

Because of the interference of the inversion spectrum with the rotational lines, the hot band transitions and the broad dimer spectrum, it is difficult to accurately determine the line-shape of the inversion lines and from this to derive the molecular response time as introduced in section IV. Figure 11a gives an example for a measured pulse (dots) transmitted through 3000 hPa of ammonia vapor at 380 mm cell length and 365 K vapor temperature, which is compared with a calculated pulse (solid line) based on the new molecular response line-shape theory and assuming a response time of $\tau_C = 80$ fs. Figure 11b shows the respective measured absorption (solid line) together with calculations of the rotation-inversion spectrum including the hot band transitions, the broad dimer absorption and assuming a response time of $\tau_C = 5$ ps (lower dotted curve) and a response time of zero (upper dash−dotted curve) representing the van Vleck−Weisskopf case. From fits to the measurements we get best consistency for $\tau_C = 80$ fs (dashed curve). The respective absorption only caused by inversion and directly representing the inversion line-shape is represented in Figure 11c for the three cases with the molecular response time $\tau_C = 5$ ps (lower dotted curve), for $\tau_C = 0$ ps (upper dash−dotted curve), and for $\tau_C = 80$ fs (dashed line).

However, it is to be noted that with only minor reduction in quality the measurements can also be fitted by a response time between zero and 150 fs, if the dimer absorption is slightly reduced or increased. As long as this background absorption cannot be determined independently or cut out, e.g., by measuring at still higher temperatures, we can only specify this line-shape parameter τ_C with an uncertainty of about 100%. The differences between the van Vleck−Weisskopf theory and our theory with τ_C only 80 fs can be observed only for large detunings, while the theories are almost indistinguishable at low frequencies. For all fits, we assumed the same molecular response time for both the inversion and the rotation transitions.

From a simple model for the response of molecules that are colliding in the presence of an electric field, it is expected that the response time scales inversely with the molecular moment of inertia. Despite the large uncertainty of this parameter a comparison with measurements on methyl halides[13] indicates that this expectation is well supported.

THz Time-Domain Spectroscopy on Ammonia

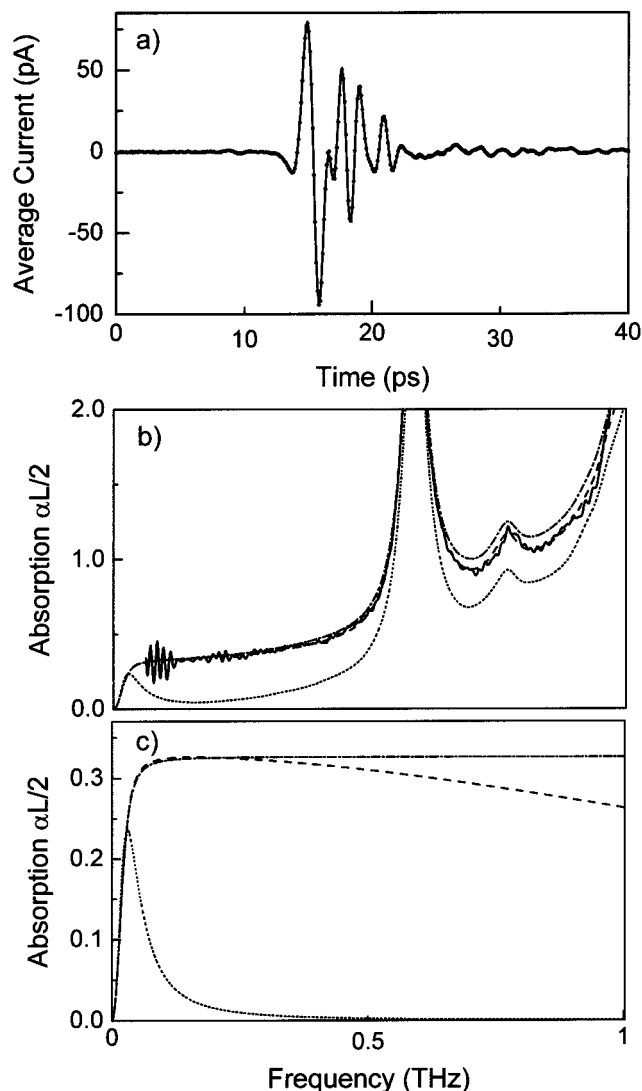*J. Phys. Chem. A, Vol. 105, No. 25, 2001* **6047**

Figure 11. (a) Measured pulse (dots) transmitted through 3000 hPa ammonia vapor at 380 mm cell length and 365 K vapor temperature. The solid line represents the calculated pulse based on the new molecular response line-shape theory with $\tau_C = 80$ fs. (b) Measured absorption (solid line) compared with calculations of the rotation–inversion spectrum using the molecular response line-shape for $\tau_C = 5$ ps (lower dashed curve), for $\tau_C = 0$ ps (upper dash–dotted curve) and for $\tau_C = 80$ fs (dashed line) almost coincident with the solid line. (c) Calculated absorption of the inversion spectrum using the molecular response line-shape for $\tau_C = 5$ ps (lower dotted curve), for $\tau_C = 0$ ps (upper dash–dotted curve) representing the van Vleck–Weisskopf case, and for $\tau_C = 80$ fs (dashed line).

Our measurements present some additional insight and discrepancies compared to the results of Bleaney and Loubser[2] or Walter and Hershberger[25] e.g., our experiments do not show zero inversion frequency at pressures of 2 atm or more. But the main difference between our measurements and the older data is that the THz experiments continuously cover the inversion spectrum as well as part of the rotation spectrum and therefore allow for observations over a wide spectral range, while the microwave experiments[2,25] were restricted to fixed frequencies within a limited frequency range. The broad spectrum measured using THz spectroscopy makes it possible to distinguish (with some restriction) between different line-shapes, and the results demonstrate the significance of the molecular response theory to overcome the nonphysical high-frequency absorption of the van Vleck–Weisskopf and Debye theory.

VI. Conclusion

Using the powerful technique of THz-TDS, we have experimentally and theoretically studied the absorption and dispersion of ammonia vapor. Our measurements showed small deviations from the rotation-inversion spectrum which originate from transitions in the ν_2 hot band and from the $(NH_3)_2$ dimer. We have investigated the molecular tunneling in ammonia and expanded our new molecular response theory to apply to the inversion spectrum of this molecule. This line-shape theory originally developed for the rotation spectrum, includes the molecular response of polar molecules to an external electric field over the duration of a collision and unifies the basic collision theories of Lorentz, van Vleck–Weisskopf and Debye, where the molecular response time τ_C acts as the control parameter. The calculated absorption and dispersion based on this theory fits the measurements over the full spectral range of the THz spectrum and allows to determine a response time τ_C of the order of 100 fs.

References and Notes

(1) Townes, C. H.; Schawlow, A. L. *Microwave Spectroscopy*; Dover Publications Inc.: New York, 1975.

(2) Bleaney, B.; Loubser, J. H. N. *Proc. Phys. Soc. A* **1950**, *63*, 483.

(3) Urban, S.; Spirko, V.; Papousek, D.; Kauppinen, J.; Belov, S. P.; Gershtein, L. I.; Krupnov, A. F. *J. Mol. Spectrosc.* **1981**, *88*, 274.

(4) Birnbaum, G.; Buechele, A.; Jiang, T.; Orton, G. S.; Hadzibabic, Z.; John, G. R. *J. Quant. Spectr. Radiat. Transfer* **2000**, *64*, 47.

(5) van Exter, M.; Fattinger, Ch.; Grischkowsky, D. *Opt. Lett.* **1989**, *14*, 1128.

(6) Grischkowsky, D.; Keiding, S.; van Exter, M.; Fattinger, Ch. *J. Opt. Soc. Am. B* **1990**, *7*, 2006.

(7) Katzenellenbogen, N.; Grischkowsky, D. *Appl. Phys. Lett.* **1991**, *58*, 222.

(8) Harde, H.; Keiding, S.; Grischkowsky, D. *Phys. Rev. Lett.* **1991**, *66*, 1834.

(9) Harde, H.; Grischkowsky, D. *J. Opt. Soc. Am. B* **1991**, *8*, 1642.

(10) Harde, H.; Katzenellenbogen, N.; Grischkowsky, D. *J. Opt. Soc. Am. B* **1994**, *11*, 1018.

(11) Harde, H.; Katzenellenbogen, N.; Grischkowsky, D. *Phys. Rev. Lett.* **1995**, *74*, 1307.

(12) Harde, H.; Cheville, R. A.; Grischkowsky, D. *J. Phys. Chem. A* **1997**, *101*, 3646.

(13) Harde, H.; Cheville, R. A.; Grischkowsky, D. *J. Opt. Soc. Am. B* **1997**, *14*, 3282.

(14) van Vleck, J. H.; Weisskopf, V. F. *Rev. Mod. Phys.* **1945**, *17*, 227.

(15) Lorentz, H. A. *Proc. Amst. Akad. Sci.* **1906**, *8*, 591.

(16) Jin, Y. H.; Zhang, X.-C. *J. Nonlin. Opt. Phys., & Mater.* **1995**, *4*, 459.

(17) Dowling, J. M. *J. Mol. Spectrosc.* **1968**, *27*, 527.

(18) Debye, P. *Polar Molecules*; Chemical Catalog Company: New York, 1929; Chapter V.

(19) Brown, L. R.; Peterson, D. B. *J. Mol. Spectrosc.* **1994**, *168*, 593.

(20) Belov, S. P.; Krupnov, A. F.; Markov, V. N.; Mel'nikov, A. A.; Skvortsov, V. A.; Tret'Yakov, M. Yu. *J. Mol. Spectrosc.* **1983**, *101*, 258.

(21) Anderson, P. W. *Phys. Rev.* **1949**, *75*, 1450.

(22) Rothman, L. S.; Rinsland, C. P.; Goldman, A.; Massie, S. T.; Edwards, D. P.; Flaud, J.-M.; Perrin, A.; Camy-Peyret, C.; Dana, V.; Mandin, Y.-Y.; Schroeder, J. W.; Gamache, R. R.; Wattson, R. B.; Yoshino, K.; Chance, K. R.; Jucks, K. W.; Brown, L. R.; Nemtchinov, V.; Varanasi, P. *Proc. SPIE* **1998**, *3375*, 123.

(23) Nelson, D. D., Jr.; Fraser, G. T.; Klemperer, W. *J. Chem. Phys.* **1985**, *83*, 6201.

(24) Olthof, E. H. T.; van der Avoird, A.; Wormer, P. E. S. *J. Chem. Phys.* **1994**, *101*, 8430.

(25) Walter, J. E.; Hershberger, W. D. *J. Appl. Phys.* **1946**, *17*, 814.